Anthropogenic carbon inventory in the Gulf of Cádiz

Susana Flecha[a,*], F. F. Pérez[b], Gabriel Navarro[a], Javier Ruiz[a], Irene Olivé[c], Susana Rodriguez-Galvez[a], Eduardo Costas[d] and I. Emma Huertas[a]

[a]Instituto de Ciencias Marinas de Andalucía CSIC, Polígono Rio San Pedro, E-11519, Spain.

[b]Instituto de Investigaciones Marinas, CSIC, Eduardo Cabello 6, E-36208 Vigo, Spain.

[c]Departamento de Biología, Universidad de Cádiz, Campus Universitario Rio San Pedro, E-11510, Spain.

[d]Facultad de Veterinaria, Universidad Complutense de Madrid. Avenida Puerta de Hierro s/n, 28040, Madrid, Spain.

***Corresponding author**

Email address: susana.flecha@icman.csic.es (Susana Flecha)

Abstract

The North Atlantic is the most important sink for atmospheric CO_2 although there still remain uncertainties about the total amount stored by this region and the contribution of the anthropogenic CO_2 (C_{ANT}) that is exchanged between the Mediterranean Sea and the Atlantic Ocean. During the P_3A_2 cruise performed in October 2008 throughout the oceanic area covered by the Gulf of Cádiz and the Strait of Gibraltar, which channelizes the water exchange between the Atlantic and the Mediterranean, extensive measurements of the carbon system parameters (pH, total alkalinity and total inorganic carbon) and others related (dissolved oxygen and nutrients) were carried out to analyse their distribution in the area. In order to study the C_{ANT} spatial variability, three observational methods for C_{ANT} concentration assessment (φC_T^o, ΔC^* and TrOCA) were applied. The three water masses identified in the area, North Atlantic Central Water (NACW), North Atlantic Deep Water (NADW) and Mediterranean Outflow Water (MOW), were shown to contain different C_{ANT} concentration. NADW exhibited the lowest C_{ANT} levels whereas NACW was the most C_{ANT} enriched. Data also indicate a net import of C_{ANT} from the Atlantic towards the Mediterranean through Gibraltar.

Specific C_{ANT} inventories showed that MOW contributes in 8-12% to the total specific C_{ANT} inventory of the Gulf of Cádiz.

Keywords

Anthropogenic CO_2, Carbon storage, Water masses, Gulf of Cádiz, Strait of Gibraltar, Mediterranean Sea.

1. Introduction

Since the late 18th Century, carbon dioxide (CO_2) concentration in the atmosphere has been rising considerably, which is directly attributable to the fossil fuel burning and changes in land use (deforestation, agriculture, etc.) by human activity (IPCC, 2007). Nevertheless, atmospheric levels are lower than expected if all the CO_2 released by anthropogenic sources had remained in the atmosphere. This mismatch is due to the fact that the ocean and land biosphere have taken up a significant amount of CO_2, thus acting as sinks for the anthropogenic carbon dioxide (C_{ANT}) (Sarmiento and Gruber, 2002). It is known that the oceans represent the major of these two sinks, storing approximately 48% of the total C_{ANT} (Sabine et al., 2004). Therefore, quantifying C_{ANT} distribution and the total amount sequestered by the oceans is crucial to better understand the role of the oceans in the global carbon cycle and how they moderate climate change (IPCC, 2007). This analysis must be, however, conducted through empirical methods based on the use of different tracers since C_{ANT} can not be directly measured.

Several methods for the indirect estimation of C_{ANT} have been developed up to date. Those based in the back-calculation technique (Brewer, 1978; Chen and Millero, 1979) are quite extended as they were the first algorithms defined to assess the temporal variation experienced by the measured inorganic carbon since a water mass was originally formed. Such variation is due to the contribution of the organic matter oxidation-reduction processes and the calcium carbonate dissolution-precipitation. Gruber et al. (1996) improved the initial method that was developed for the Atlantic Ocean and defined the quasi-conservative carbon tracer ΔC^*, which reflects the uptake

of C_{ANT} and the air-sea disequilibrium present when the water mass loses contact with the atmosphere, assuming that it remains constant over time. A more recent method for C_{ANT} computation is the TrOCA approach, which was originally proposed by Touratier and Goyet (2004b) and further improved by Touratier et al (2007). This technique considers a quasi-conservative tracer TrOCA, which combines Oxygen, inorganic Carbon, and Total Alkalinity and that is based on the conservative NO tracer (Broecker, 1974; Ríos et al., 1989; Touratier and Goyet, 2004a). Both the TrOCA approach and the ΔC* technique assume that below the mixed layer, the decomposition of organic matter follows a constant Redfield stoichiometry and that today's air-sea CO_2 disequilibrium is identical to the one present in pre-industrial times. Current studies have indicated that the TrOCA method considerably overestimates anthropogenic carbon concentrations (Yool et al., 2011). Nevertheless, method has been still applied in our work in order to compare the data obtained with the previous results shown by Aït-Ameur and Goyet (2006) in the Gulf of Cádiz. A new parameterization , has been lately proposed by Vazquez-Rodriguez et al. (2009a) , the so-called φC_T^o method, which represents a revision of ΔC* and it is aimed at improving the assessment of C_{ANT} inventory in the Atlantic Ocean. The main contribution of the φC_T^o method is the use of sub-surface layer data (100-200m) to reconstruct water mass formation conditions, thereby obtaining better estimates of preformed properties instead of using other transient traces, such as CFC, to quantify the effect of the air-sea disequilibrium on the C_{ANT} concentration.

However, regardless of the method considered for C_{ANT} calculation, several studies have confirmed that the North Atlantic is the most important sink for atmospheric CO_2 (Takahashi, 2009; Sabine et al., 2004), although there still remain uncertainties about the total amount stored by this region. In the past, the contribution of areas such as marginal seas, semi-enclosed seas and continental shelves to the global C_{ANT} inventories was understudied. Nevertheless, recent studies that evaluate the CO_2 sink capacity of these areas have demonstrated that they take up larger amounts of C_{ANT} which contribute significantly to the overall global C_{ANT} inventories (Tanhua et al., 2009; Schneider et al., 2010; Lee et al., 2011). Therefore, there is a clear research need to accurately quantify the amount of carbon that is captured by the total coastal ocean and subsequently transferred to the open sea. In response to this increasing interest, several studies have been carried out in the coastal area comprised by the Gulf of Cádiz and the

Strait of Gibraltar (Aït-Ameur and Goyet, 2006; Huertas et al., 2006; 2009; de la Paz et al., 2008, 2011; Ribas-Ribas et al., 2011). Data attained by these studies indicate that this region acts as a moderate sink for atmospheric CO_2 and that a net export of total inorganic carbon occurs from the Mediterranean to the Atlantic. On the other hand, there have been contradicting results about the concentration of C_{ANT} that is exchanged between both basins (Aït-Ameur and Goyet, 2006; Huertas et al., 2006; 2009). These discrepancies may be related to the different methods used to obtain C_{ANT} concentrations, as the TrOCA approach seems to overestimate Mediterranean waters anthropogenic carbon levels. Therefore, the main aim of this work was to examine the spatial variability of the C_{ANT} in the Gulf of Cádiz considering all the water masses present in the area, in order to gain insights on the role of the Strait of Gibraltar in the fluxes of the anthropogenic carbon. This analysis was performed by applying all the aforementioned C_{ANT} calculation techniques not only with the aim at comparing the results provided by the different methods currently available and generally applied but also to allow the comparison with data reported in the past in this geographic zone by using the TrOCA approach.. Furthermore, a C_{ANT} inventory for the whole area is provided, with the relative contribution of the outflow of Mediterranean water to the specific inventory being also given.

1.1 Study Area

The oceanic area covered by the Gulf of Cádiz and the Strait of Gibraltar, located southwest of the Iberian Peninsula (Fig. 1), plays a relevant role in the general circulation of the North Atlantic owing to the channelization of the water exchange between the Atlantic and the Mediterranean Sea (Péliz et al., 2009; Criado-Aldeanueva et al., 2009). Thus, the entrainment of North Atlantic Central Water (NACW) by the Mediterranean outflow (MOW) as it descends the northern slope of the Gulf of Cádiz markedly contributes to the generation of the Azores current and also drives upper slope currents in the basin (Péliz et al., 2009).

The Strait of Gibraltar is a narrow and shallow channel with an east-west orientation of a minimum width of 14 km (the Tarifa Narrows, TN in Fig. 1) and an average depth of 600 m, although the main sill of the Strait (Camarinal Sill, CS in Fig. 1) is hardly 300 m depth and imposes a severe constrain for the ventilation of deep Mediterranean waters. On the other hand, the adjacent Gulf of Cádiz is divided into two different portions by

Cape Santa Maria (CSM) (Fig. 1), with each of these halves presenting different topographic characteristics. West of CSM, the continental shelf is narrow and the sea bottom is characterized by the presence of submarine canyons. On the contrary, east of the cape the continental shelf becomes wider and hosts important rivers whose mouths provide the basin with freshwater and nutrients that control primary production in the coastal fringe (Prieto et al., 2009). As underlined above, the circulation of water masses in the Gulf is markedly controlled by the Mediterranean-Atlantic exchange that takes place in the Strait of Gibraltar. The saltier and denser MOW moves westwards in depth, being distinguishable through two main cores centred at about 800 and 1200 m depth. This subdivision is probably due to the bottom topography that channels different branches along certain isobaths (Ambar and Howe, 1979; Serra and Ambar, 2002). In addition, a third shallower core can be detected at depths around 500 m in the continental shelf (Ambar et al., 2002). In contrast, Atlantic waters flow eastward to the Mediterranean Sea, occupying the upper layer in the Strait of Gibraltar. The confluence of both water bodies determines the two layer circulation scheme found in the Strait. The exchange of waters is mainly driven by the water deficit occurring in the Mediterranean basin, as the excess of evaporation over precipitation and river run off forces the Atlantic jet to progress towards the Mediterranean Sea to compensate water losses (Bryden et al., 1994).

The presence of NACW in the area is evident below 100 m depth, as described in previous studies (Navarro et al., 2006). This water mass has been categorized in two varieties, such as the warmer Eastern North Atlantic Central Water of subtropical origin ($ENAC_t$) and the colder subpolar Eastern North Atlantic Central Water ($ENAC_s$) (Ríos et al., 1992; Pollard et al., 1996; Pérez et al., 2001; Alvarez et al., 2005). At shallower depths, NACW is modified by the atmospheric interaction and it has been defined as North Atlantic Surface Water (Gascard and Richez, 1985). Furthermore, the North Atlantic Deep Water (NADW) can be found at depths greater than 1500 m (Emery and Meincke, 1986; Alvarez et al., 2005) associated with a depth-decreasing thermohaline properties (Ambar et al., 2002).

2. Material and Methods

2.1. Sampling

The P_3A_2 oceanographic cruise was conducted on board the R.V. Hespérides from the 04^{th} to the 22^{nd} of October 2008. A macroscale study was completed in a sampling grid composed by 45 stations distributed from CSM to the Strait of Gibraltar (Fig.1). At each station CTD profiles were obtained with a SeaBird SBE 911, followed by collection of water samples with rosette at different depths (from 5 m up to ~2000 m or bottom depth) in order to determine the spatial distribution of several biogeochemical variables, such as total alkalinity, pH, dissolved oxygen and inorganic nutrients (nitrite, nitrate, phosphate and silicate).

2.2. Measurements

2.2.1. Total Alkalinity

Total alkalinity (A_T) was measured with a Metrohm 794 Titroprocessor following the method described by Mintrop et al. (2000). Water samples were taken from the Niskin bottles and preserved in 500 mL borosilicate bottles poisoned with 100 µL of $HgCl_2$ saturated aqueous solution and kept until subsequent onboard and onshore analysis. Accuracy of A_T determination was calculated from regular measurements of 2 batches (batch # 85 and 89) of Certified Reference Material (CRM supplied by Prof. Andrew Dickson, Scripps Institution of Oceanography, La Jolla, CA, USA), resulting in ±2 µmol kg^{-1}.

2.2.2 pH

pH was measured following the spectrophotometric method of Clayton and Byrne (1993) using m-cresol purple as the indicator, and consequently, the scale used was the total scale. Samples were collected directly from the rosette in 10 cm path-length optical glass cells and measurements were carried out onboard with a Shimadzu UV-2401PC spectrophotometer containing a 25ºC-thermostated cells holder.

This method has been proved to have an accuracy of ±0.003 pH units (Clayton and Byrne, 1993). Accuracy of our pH determinations was calculated from regular measurements of 2 CRMs batches (# 85 and # 89). From both pH and A_T values, the concentration of inorganic carbon (C_T) was calculated using the dissociation constants from Mehrbach et al. (1973) refitted by Dickson and Millero (1987).

2.2.3 Dissolved Oxygen

Dissolved oxygen was determined following the Winkler method (Winkler, 1888). Seawater was taken in sealed flasks directly from the Niskin bottles and stored in darkness for at least 24 h. Analysis was performed by potentiometric determination using a Metrohm 794 Titroprocessor, with an estimated error of ±1 μmol kg^{-1}.

2.2.4 Nutrients

Two 5 mL replicates of filtered seawater (GF/F Whatman filters) were taken and stored at -20ºC until onshore laboratory analysis. Concentration of NO_2, NO_3, PO_4 and Si $(OH)_4$ were obtained following the techniques described by Grasshoff et al. (1983) with a Skalar San^{++}System autoanalyser.

2.3. Calculation of C_{ANT} concentration

As already indicated, several methods were applied to calculate C_{ANT} in the study region: the TrOCA approach with the set of parameters proposed by Touratier and Goyet (2004b) and with the latter improvements of Touratier et al. (2007), designated here as $TrOCA_{2004}$ and $TrOCA_{2007}$ respectively; the back-calculation technique (ΔC^*) and the φC_T^o method. The original $TrOCA_{2004}$ parameterization (Touratier and Goyet 2004b) was exclusively used to compare the results attained in this study with previous estimations reported in the area based on such method (Aït-Ameur and Goyet, 2006). Regardless of the calculation technique applied, the first 100 m of the water column were excluded for C_{ANT} assessments and hence only data obtained in stations with waters deeper than 100 m were considered.

C_{ANT} (TrOCA) has been computed using the following relationship

$$C_{ant}(TrOCA_{2004;2007}) = \frac{TrOCA - TrOCA^{\circ}}{a}, \quad (2)$$

where TrOCA represents a semi-conservative tracer based on the Redfield oxidation-reduction ratios of organic matter, calculated as follows:

$$TrOCA_{2004} = O_2 + aC_T - 0.6A_T, TrOCA_{2007} = O_2 + a(C_T - 1/2\,A_T), \quad (3, 4)$$

and $TrOCA^o$ is defined as the pre-industrial TrOCA:

$$TrOCA°_{2004} = 1505.04e^{(-\theta/89.04)}, TrOCA°_{2007} = e^{(7.511+(1.087\times10^{-2})\theta-(7.81\times10^{-5}/A_T^2))}, \quad (5, 6)$$

where the constant *a* is equal to 1.2 and 1.279 for the $TrOCA_{2004}$ and the $TrOCA_{2007}$ parameterizations respectively.

For the back-calculation technique, the following equation was used:

$$C_{ANT}(\Delta C^*) = C_T - AOU/R_C - 1/2(\Delta A_T + AOU/R_N) - C^\circ_{T278} - \Delta C_{dis}, \quad (7)$$

where C_T is the dissolved inorganic carbon concentration of the sample expressed in μmol kg^{-1} and AOU stands for Apparent Oxygen Utilization, which was calculated using the oxygen saturation equation of Benson and Krause (1984). The stoichiometric coefficients R_C ($-\Delta O_2/\Delta C$) =1.45 and R_N ($-\Delta O_2/\Delta N$) =10.6 of Anderson and Sarmiento (1994) were taken. AOU/R_C corresponds to the C_T increase due to organic matter oxidation and $½(\Delta A_T+AOU/R_N)$ accounts for the C_T change due to $CaCO_3$ dissolution-precipitation, where $\Delta A_T = A_T - A^\circ_T$ is the total alkalinity variation since the water mass was formed. Preformed alkalinity (A°_T) and the disequilibrium term that stands for the air-sea CO_2 difference expressed in terms of C_T (ΔC_{dis}), were obtained for each water sample from the mixing proportion of the different water masses. This was carried out by an extended optimum multiparameter analysis (eOMP) (Poole and Tomczak, 1999). The A°_T type values for the Atlantic Waters were calculated using the approach proposed by Perez et al. (2002) while those by Rhein and Hinrichsen (1993) and Santana-Casiano et al. (2002) were used for the MOW. C°_{T278} represents the C_T in equilibrium with the preindustrial atmospheric CO_2 molar fraction of 278 ppm and was calculated using the dissociation constants of Merbach et al. (1973) refitted by Dickson and Millero (1987). ΔC_{dis} for both NACW and NADW was considered to be −12±5 μmol kg^{-1} and -10±8 μmol kg^{-1}, respectively (Lee et al. 2003) whereas for the MOW ΔC_{dis} was obtained from Huertas et al. (2009), which sets ΔC_{dis} in 0±5 μmol kg^{-1} using the CFC data given by Rhein and Hinrichsen (1993). As for the $\varphi C_T{}^o$ method (Vazquez-Rodriguez et al. 2009a), new A°_T and ΔC_{dis} parameterizations were included in the equation based on a 100-200 m depth surface layer that is taken as a reference for reconstructing water mass formation conditions. Accordingly, the NO and PO conservative tracers defined by Broecker (1974) and the preformed silicate ($S_i{}^o$) provided by Perez et al. (2002) were used. For the term ΔC_{dis}, a distinction depending on different potential temperature (θ) intervals was made in the case of Atlantic waters

whereas for the MOW (S>36.5), A_T° and ΔC_{dis} were obtained by eOMP analysis. The different water masses found in the area were defined in the eOMP analysis by several water types (WT): WT1 and WT2 correspond to the two different varieties of NACW (ENACWt and ENACWs, respectively), WT3 designs NADW and WT4 marks MOW, as summarized in Table 1.

Therefore, the C_{ANT}^{φ} calculation equation can be summarized as follows

$$C_{ANT}(\varphi C_T^0) = \frac{\Delta C^* - \Delta C_{dis}^t}{1 + \varphi \left| \Delta C_{dis}^t \right| / C_{ant}^{sat}}, \quad (8)$$

with $\Delta C^* = C_T - AOU/R_C - \Delta Ca - C_{T278}^\circ$ where ΔCa is the term related to the $CaCO_3$ dissolution, since $\Delta Ca = 0.5(PA_{T,observed} - PA_T^\circ)$ with $PA_T = A_T + NO_3 + PO_4$ and $PA_T^\circ = A_T^\circ + NO_3^\circ + PO_4^\circ$, being $NO_3^\circ = NO_3 - AOU/9$ and $PO_4^\circ = PO_4 - AOU/135$. The O_2:N=9 and O_2:P=135 Redfield ratios proposed by Broecker (1974) were taken. Furthermore, in the $C_{ANT}(\varphi C_T^0)$ equation, the constant term φ is a proportionality factor and equals the ratio between the temporal variability of the air-sea disequilibrium of CO_2 from the time of pre-industrial water mass formation to the time "t" ($\Delta\Delta C_{dis}$), with the disequilibrium at the time "t" being ΔC_{dis}^t. Finally, C_{ant}^{sat} represents the anthropogenic carbon saturation referred to a $xCO_{2\ air}$ of 384 ppm, which is taken from measurements performed at the meteorological station of the Lampedusa (Italy, Cooperative Air Sampling Network of the NOAA/ESRL Global Monitoring Division) and it is included to account for the effects of temperature and salinity on the solubility of C_{ANT} in the different water masses.

In order to estimate the uncertainty associated to the C_{ANT} calculation techniques an error propagation analysis was conducted for each method. The error for C_{ANT} assessments using the $TrOCA_{2004}$ and the $TrOCA_{2007}$ parameterizations were ±5.3 µmol kg^{-1} and ±5.5 µmol kg^{-1}, respectively; ±6.1 µmol kg^{-1} when the ΔC^* technique was applied and ±5.6 µmol kg^{-1} in the case of the φC_T^o method. In previous works, the overall estimated C_{ANT} uncertainties ranged from ±3 to 5.9 µmol kg^{-1} for the $TrOCA_{2004}$ approach (Touratier et al. 2004b), ±6.2 for the $TrOCA_{2007}$ parameterization (Touratier et al. 2007), ±9 for the ΔC^* technique (Gruber et al. 1996) and ±5.2 for the φC_T^o method (Vazquez-Rodriguez et al. 2009a).

3. Results and Discussion

3.1. Water masses and carbon system parameters in the study area.

Three water masses were clearly identified in the Gulf of Cádiz according to their different thermohaline properties (Fig.2a): NACW, NADW and MOW. NACW, located above 500 m depth, was well defined with a temperature range from 11 to 18 ºC and salinity values around 35.5-36.3. This water mass showed a linear behaviour for the isopicnals interval of 26.6 kg $m^{-3} \leq \sigma_\theta \leq 27.3$ kg m^{-3}, as described in Criado-Aldeanueva et al. (2006). The MOW signal could be detected throughout the entire study area and up to 1500 m depth (Figs. 5f, 6f). In particular, MOW in the Strait of Gibraltar is defined by a salinity of 38.5 and a temperature value of 13ºC (Figs. 4b-c) (Gascard and Richez 1985; Garcia-Lafuente et al. (2007) whereas in the Gulf of Cadiz was clearly evident at a pressure of around 1000 dbar because of a salinity and potential temperature increase (Fig. 3b-c). This signal corresponds to the lower core of the MOW (Fig. 5f) (Ambar and Howe, 1979; Serra and Ambar, 2002). In contrast, NADW was found in a reduced number of deep stations (depth>1500 m) located in the southwestern part of the surveyed region (Fig. 5e, 6e). This water mass was previously described in the Iberian Basin by Alvarez et al. (2005) with salinity and temperature values around 34.9 and 2.4 ºC, respectively. In our study, NADW was slightly modified as it showed salinity and temperature values around 35ºC and 5ºC respectively (Figs. 3b-c, 4b-c).

All the water masses identified were also characterized by specific carbonate properties, as the variability of A_T, AOU and C_T (Figs. 2b-d) was well correlated with the distribution of the different water masses. Due to the shallower location of the NACW (Figs. 5d, 6d), its thermohaline properties suffer modifications caused by the air-sea interactions and river discharges (Criado-Aldeanueva et al., 2009), which resulted in the highest variability found for these parameters within the same water mass (Figs. 2b-d). Moreover, the pattern of AOU allowed to distinguish the presence of the two varieties of the NACW described in the area: the $ENAC_t$, which is oxygen saturated, was thereby characterized by the lowest AOU levels at about 6 µmol kg^{-1} (Fig. 2c), coinciding with previous reports (Aït-Ameur and Goyet, 2006) and the $ENAC_s$ which is located below the former, and exhibited an increase in the AOU levels (Fig. 2c). Perez et al. (2001)

attributed this deeper AOU maximum to the remineralization of organic matter in the African coast linked to the northwest African upwelling system. Within the NACW layer, A_T and C_T showed intermediate levels in relation to the total measurements, with average values around 2360±2 and 2130±2 µmol kg^{-1}, respectively (Figs. 2b,d, 3d-e, 4d-e). As expected, the highest A_T (2576±6 µmol kg^{-1}) and C_T contents (2317 ±5 µmol kg^{-1}) were found in the MOW located in the western side of the Strait (Figs. 2b-d). In the vertical sections of the N-S and W-E transects, the biogeochemical properties of the MOW were also evident in the lower core (Figs. 3d-f, 5f) and in the western part of the Strait (Figs. 4d-f, 6f), with values that coincide with those reported by Aït-Ameur and Goyet (2006) and Huertas et al. (2009) in the area. The elevated AOU levels of about 80 µmol kg^{-1} within this layer indicated the lower oxygen concentrations present in the MOW due to the active remineralisation of organic matter occurring in the Mediterranean basin (Huertas et al., 2009).

On the other hand, the A_T and C_T signatures inside the NADW showed lower values equivalent to 2329±7 µmol kg^{-1} and 2167±2 µmol kg^{-1}, respectively (Fig. 2b, d). In fact, data plotted in the vertical sections of the transects revealed a decrease of these properties with depth (Figs. 3d-e, 4d-e) due to the presence of this water mass (Figs. 5e, 6e). It is also worth mentioning that the high AOU values (~80 µmol kg^{-1}) detected in this water mass (Fig. 2c) can be related to the ageing of water masses that results in a simultaneous increase in AOU, nitrate and phosphate owing to the mineralization of organic matter (van Aken, 2000).

The linear relationship between salinity and A_T obtained for the whole region was calculated at a salinity reference of 35 in order to remove spatio-temporal changes. The equation obtained (A_T= [(84.3±1.6)*(S-35)-(2277±2), r^2=0.95, n=156] indicated that mixing is the main controlling factor for the A_T distribution, in a similar way as in Santana-Casiano et al., (2002) and Huertas et al., (2009). These authors reported linear relationships of A_T=2353(±0.4) +92.28(±0.31) (S-36.0) (r^2=0.998) and A_T =92.98×S-993 (r^2=0.989) for the Gulf and the Strait, respectively. The new relationship attained here was based on data collected in a wider area, which is influenced by the presence of water masses with lower salinity, such as the NADW, which is absent in the Strait. This circumstance may explain the reduction in the slope and the slight diminution in the correlation coefficient compared to the ones reported by previous works.

3.2. C_{ANT} distribution

The vertical distribution of C_{ANT} calculated using the $TrOCA_{2007}$, the ΔC^* and the φC_T^o methods is plotted in Fig. 5 for a N-S section and in Fig. 6 for an E-W section. The red transects indicated in Figs. 3a and 4a were chosen as representatives of all the legs sampled.

In the N-S section, the spatial pattern of C_{ANT} was similar regardless of the method used for computation, as all of them resulted in a vertical decreasing gradient (Figs. 5a-c). The maximum concentrations of C_{ANT} were consistently located in 100 m depth waters (50-60 µmol kg^{-1}), where the highest proportion of NACW was present (Fig. 5d). In contrast, the lowest C_{ANT} values were found at depths below 1500 dbar (Figs. 5a-c) due to the slight C_{ANT} penetration into the domain of the NADW (Fig. 5e), as described by Ríos et al., 2001). Within this layer, C_{ANT} concentrations showed concordant values between 9 and 12 µmol kg^{-1} for all the methods applied (Figs. 5a-c). The higher salinity zone found at about 1000-1200 dbar in the continental slope (Fig. 3b) and corresponding to the lower MOW core (Fig. 5f), was characterized by an increase in C_{ANT} concentration, especially when the $TrOCA_{2007}$ parameterization was used (Fig. 5c), resulting in concentrations of 50 µmol kg^{-1} approximately.

In the E-W section, the distribution of C_{ANT} (Figs. 6a-c) revealed a similar trend for the three parameterizations used except for that obtained in the Strait of Gibraltar with the $TrOCA_{2007}$ approach. According to this method, the MOW located in the Strait was characterised by the highest C_{ANT} content (Fig.6c), particularly waters with salinities >37.5 (Fig.4b). C_{ANT} $TrOCA_{2007}$ concentration in the easternmost part displayed values around 63±1 µmol kg^{-1} (Fig.6c), which declined westwards and upwards in the water column. Moreover, when the original $TrOCA_{2004}$ parameterization was applied in order to compare with previous estimates (not shown), MOW exhibited average C_{ANT} levels of 92±1 µmol kg^{-1}, whereas NADW and NACW showed 24 ±4 µmol kg^{-1} and 55 ±1 µmol kg^{-1} in good agreement with the values reported by Aït-Ameur et al. (2006). Therefore, comparing both TrOCA parameterizations, the initial $TrOCA_{2004}$ method yielded values around 40% higher than those attained by the technique subsequently refined (Fig. 6c).

On the contrary, when both the φC_T^o and ΔC^* methods were applied in the Strait, higher C_{ANT} concentrations were detected within the NACW located in the upper layer of the

water column, with a decreasing vertical pattern being also evidenced (Figs. 6a, c). This discrepancy can be explained by the nature of the equations, as the general TrOCA approach applies a global formula that is a function exclusively of θ, O_2 and A_T measured *in situ* (Eqs. 3, 4) whereas the back-calculation techniques include the computation of the pre-industrial carbon level and the disequilibrium due to the air-sea CO_2 difference (Eqs. 5, 6), which are adapted regionally considering the formation of each particular water mass. This feature was already highlighted in the early analysis performed in the Strait by Huertas et al., (2009). In the rest of the surveyed region, the ranges of C_{ANT} concentration within the NACW and NADW coincide with those observed in the N-S transect independent of the approach applied.

3.3. C_{ANT} inventory

The specific inventory of C_{ANT} for the entire area was determined by integrating the average vertical C_{ANT} profiles attained at each station from surface down to the bottom depth. Because C_{ANT} concentrations were calculated from 100 dbar to the sea bottom, the surface layer above this depth was assumed to contain a constant C_{ANT} level equal to that present at this upper limit, which also marks the winter mixing layer for Atlantic subtropical waters (Vázquez-Rodríguez et al., 2009a). This artefact for inventory computations allows to avoid the influence of the seasonal biogeochemical variability on surface C_{ANT} estimates (Lo Monaco et al., 2005; Vázquez-Rodríguez et al., 2009a). Specific inventories calculated in the region by the different techniques showed small differences (Table 2). Nevertheless, should be taken into account in the inventory results obtained that they represent average values for the totality of the waters masses present in the area (not shown). As is shown in the Table 2, the initial $TrOCA_{2004}$ method yielded the highest specific inventory with 38.0±3.1 mol C m^{-2}, whereas the rest of calculation techniques resulted in similar values, with the minimum provided by the φC_T^o method equivalent to 33.5±3.2 mol C m^{-2}. Estimates were statistically analyzed by a student´s t test and averaged results obtained showed no statistical differences between the different methods applied.

These values are comparable to the specific inventory presented by Lee at al. (2011) for the East/Japan Sea and equal to 34±5.1 mol C m^{-2}. The specific inventory for the entire Eastern North Atlantic comprised in the 30ºN-40ºN latitude band, where our study area

is contained, has been estimated in 66.2 mol C m^{-2}, using the ΔC^* (Lee et al., 2003) and in 75 mol C m^{-2} with the φC_T^o method (Vázquez-Rodríguez et al., 2009b) . The differences between such estimates and those obtained here are due to the lower volume of water contained in the surveyed region in relation to that of the Eastern North Atlantic, as the vertical interpolation markedly depends of the water column volume.

Since the main differences in the C_{ANT} contents observed in our study were related to the presence of the Mediterranean waters (Figs. 6a-c), the contribution of the MOW to the specific C_{ANT} inventory was also calculated with each technique. Results summarized in Table 2 indicate that the Mediterranean supplies 8% of the total C_{ANT} specific inventory when the φC_T^o and ΔC^*methods were used. A small increase in this contribution (11-12 %) was attained with the two TrOCA approaches, as a result of the higher concentration of C_{ANT} assigned to the MOW by both parameterizations (Fig. 6c).

4. Conclusions

The analysis of the spatial distribution of the carbon system parameters in the area covered by the Gulf of Cádiz and the Strait of Gibraltar reflected the presence of different water masses that were characterized by distinct biogeochemical properties. The concentration of C_{ANT} calculated for each water mass according to three estimation methods resulted in small variations. The main discrepancies between the results obtained by all the methods were found in the MOW, as both TrOCA approaches seem to overestimate C_{ANT} concentration within this water mass. Accordingly, slight differences were found in the specific inventories with the exception of the value provided by the $TrOCA_{2004}$ approach. Furthermore, the quantification of the additive effect of the C_{ANT} contained in the MOW on that measured in Atlantic waters at intermediate depths has been evidenced in this study. This work also presents new data on the C_{ANT} levels present in a coastal ocean region, whose role in the capture and storage of CO_2 had been underestimated in the past. These results also represent a contribution to the North Atlantic specific carbon inventories.

5. Acknowledgments

The excellent co-operation of the crew of the BIO Hespérides is gratefully acknowledged. We also thank María Ferrer-Marco, Simone Taglialatela and Mónica

Rouco for sample collection and measurements. Funding for this work was provided by the CARBOOCEAN IP (511176GOCE) of the European Commission and by the Spanish Ministry of Sciences and Innovation through the projects CTM2005/01091-MAR and CTM2008-05680-C02-01.

6. References

Aït-Ameur, N., Goyet, C., 2006. Distribution and transport of natural and anthropogenic CO_2 in the Gulf of Cadiz. Deep-Sea Research Part II-Topical Studies in Oceanography 53, 1329-1343

Alvarez, M., Perez, F.F., Shoosmith, D.R., Bryden, H.L., 2005. Unaccounted role of Mediterranean Water in the drawdown of anthropogenic carbon. Journal of Geophysical Research-Oceans 110

Ambar, I., Howe, M.R., 1979. Observations of the Mediterranean Outflow .2. Deep circulation in the vicinity of the Gulf of Cadiz. Deep-Sea Research-Part I-Oceanographic Research Papers 26, 555-568

Ambar, I., Serra, N., Brogueira, M.J., Cabecadas, G., Abrantes, F., Freitas, P., Goncalves, C., Gonzalez, N., 2002. Physical, chemical and sedimentological aspects of the Mediterranean outflow off Iberia. Deep-Sea Research Part II-Topical Studies in Oceanography 49, 4163-4177

Anderson, L.A., Sarmiento, J.L., 1994. Redfield ratios of remineralization determined by nutrient data analysis. Global Biogeochemical Cycles 8, 65-80

Benson, B.B., Krause, D., 1984. The concentration and isotopic fractionation of oxygen dissolved in fresh-water and seawater in equilibrium with the atmosphere. Limnology and Oceanography 29, 620-632

Brewer, P.G., 1978. Direct observation of oceanic CO_2 increase. Geophysical Research Letters 5, 997-1000

Broecker, W.S., 1974. NO a conservative water-mass tracer. Earth and Planetary Science Letters 23, 100-107

Bryden, H.L., Candela, J., Kinder, T.H., 1994. Exchange through the Strait of Gibraltar. Progress in Oceanography 33, 201-248

Clayton, T.D., Byrne, R.H., 1993. Spectrophotometric seawater pH measurements- total hygrogen scale calibration of m-cresol purple ant at-sea results. Deep-Sea Research Part I-Oceanographic Research Papers 40, 2115-2129

500 Criado-Aldeanueva, F., Garcia-Lafuente, J., Navarro, G., Ruiz, J., 2009. Seasonal and
501 interannual variability of the surface circulation in the eastern Gulf of Cadiz (SW
502 Iberia). Journal of Geophysical Research-Oceans 114
503 Criado-Aldeanueva, F., Garcia-Lafuente, J., Vargas, J.M., Del Rio, J., Vazquez, A.,
504 Reul, A., Sanchez, A., 2006. Distribution and circulation of water masses in the Gulf of
505 Cadiz from in situ observations. Deep-Sea Research Part II-Topical Studies in
506 Oceanography 53, 1144-1160
507 Chen, C.T., Millero, F.J., 1979. Gradual increase of oceanic carbon dioxide. Nature 277,
508 205-206
509 de la Paz, M., Debelius, B., Macias, D., Vazquez, A., Gomez-Parra, A., Forja, J.M.,
510 2008. Tidal-induced inorganic carbon dynamics in the Strait of Gibraltar. Continental
511 Shelf Research 28, 1827-1837
512 de la Paz, M., Huertas, M.E., Padín, X.-A., Gónzalez-Dávila, M., Santana-Casiano, M.,
513 Forja, J.M., Orbi, A., Pérez, F.F., Ríos, A.F., 2011. Reconstruction of the seasonal cycle
514 of air-sea CO_2 fluxes in the Strait of Gibraltar. Marine Chemistry In Press, Corrected
515 Proof
516 Dickson, A.G., Millero, F.J., 1987. A comparison of the equilibrium-constants for the
517 dissociation of carbonic-acid in seawater media. Deep-Sea Research Part I-
518 Oceanographic Research Papers 34, 1733-1743
519 Emery, W.J., Meincke, J., 1986. Global Water Masses - Summary and Review.
520 Oceanologica Acta 9, 383-391
521 Garcia-Lafuente, J., Roman, A.S., del Rio, G.D., Sannino, G., Garrido, J.C.S., 2007.
522 Recent observations of seasonal variability of the Mediterranean outflow in the Strait of
523 Gibraltar. Journal of Geophysical Research-Oceans 112
524 Gascard, J.C., Richez, C., 1985. Water masses and circulation in the Western Alboran
525 Sea and in the Strait of Gibraltar. Progress in Oceanography 15, 157-216
526 Grasshoff, K., Ehrhard, M., Kremling, K., 1983. Determination of nutrients. In:
527 Methods of Seawater Analysis, 2nd ed. Verlag Chemie, Weinheim.
528 Gruber, N., Sarmiento, J.L., Stocker, T.F., 1996. An improved method for detecting
529 anthropogenic CO_2 in the oceans. Global Biogeochemical Cycles 10, 809-837
530 Huertas, I.E., Navarro, G., Rodriguez-Galvez, S., Lubian, L.M., 2006. Temporal
531 patterns of carbon dioxide in relation to hydrological conditions and primary production
532 in the northeastern shelf of the Gulf of Cadiz (SW Spain). Deep-Sea Research Part II-
533 Topical Studies in Oceanography 53, 1344-1362

Huertas, I.E., Rios, A.F., Garcia-Lafuente, J., Makaoui, A., Rodriguez-Galvez, S., Sanchez-Roman, A., Orbi, A., Ruiz, J., Perez, F.F., 2009. Anthropogenic and natural CO_2 exchange through the Strait of Gibraltar. Biogeosciences 6, 647-662

IPCC, 2007. Climate Change 2007: The Physical Science Basis, Contribution of Working Group I to the Fourth Assessment Report of the Intergovernmental Panel on Climate Change. Cambridge University Press, Cambridge, United Kingdom. New York, NY, USA.

Lee, K., Choi, S.D., Park, G.H., Wanninkhof, R., Peng, T.H., Key, R.M., Sabine, C.L., Feely, R.A., Bullister, J.L., Millero, F.J., Kozyr, A., 2003. An updated anthropogenic CO_2 inventory in the Atlantic ocean. Global Biogeochemical Cycles 17

Lee, K., Sabine, C.L., Tanhua, T., Kim, T.W., Feely, R.A., Kim, H.C., 2011. Roles of marginal seas in absorbing and storing fossil fuel CO_2. Energy & Environmental Science 4, 1133-1146

Lo Monaco, C., Goyet, C., Metzl, N., Poisson, A., Touratier, F., 2005. Distribution and inventory of anthropogenic CO_2 in the Southern Ocean: Comparison of three data-based methods. Journal of Geophysical Research-Oceans 110

Mehrbach, C., Culberso.Ch, Hawley, J.E., Pytkowic.Rm, 1973. Measurements of apparent dissociation-constants of carbonic-acid in seawater at atmospheric-pressure. Limnology and Oceanography 18, 897-907

Mintrop, L., Perez, F.F., Gonzalez-Davila, M., Santana-Casiano, M.J., Kortzinger, A., 2000. Alkalinity determination by potentiometry: Intercalibration using three different methods. Ciencias Marinas 26, 23-37

Navarro, G., Ruiz, J., Huertas, I.E., Garcia, C.M., Criado-Aldeanueva, F., Echevarria, F., 2006. Basin-scale structures governing the position of the deep fluorescence maximum in the Gulf of Cadiz. Deep-Sea Research Part II-Topical Studies in Oceanography 53, 1261-1281

Péliz, A., Marchesiello, P., Santos, A.M.P., Dubert, J., Teles-Machado, A., Marta-Almeida, M., Le Cann, B., 2009. Surface circulation in the Gulf of Cadiz: 2. Inflow-outflow coupling and the Gulf of Cadiz slope current. Journal of Geophysical Research-Oceans 114

Pérez, F.F., Álvarez, M., Ríos, A.F., 2002. Improvements on the back-calculation technique for estimating anthropogenic CO_2. Deep-Sea Research Part I-Oceanographic Research Papers 49, 859-875

Pérez, F.F., Mintrop, L., Llinas, O., González-Davila, M., Castro, C.G., Alvarez, M., Kortzinger, A., Santana-Casiano, M., Rueda, M.J., Ríos, A.F., 2001. Mixing analysis of nutrients, oxygen and inorganic carbon in the Canary Islands region. Journal of Marine Systems 28, 183-201

Pollard, R.T., Griffiths, M.J., Cunningham, S.A., Read, J.F., Perez, F.F., Rios, A.F., 1996. Vivaldi 1991-A study of the formation, circulation and ventilation of Eastern North Atlantic Central Water. Progress in Oceanography 37, 167-192

Poole, R., Tomczak, M., 1999. Optimum multiparameter analysis of the water mass structure in the Atlantic Ocean thermocline. Deep-Sea Research Part I-Oceanographic Research Papers 46, 1895-1921

Prieto, L., Navarro, G., Rodriguez-Galvez, S., Huertas, I.E., Naranjo, J.M., Ruiz, J., 2009. Oceanographic and meteorological forcing of the pelagic ecosystem on the Gulf of Cadiz shelf (SW Iberian Peninsula). Continental Shelf Research 29, 2122-2137

Rhein, M., Hinrichsen, H.H., 1993. Modification of Mediterranean Water in the Gulf od Cadiz, studied with hidrographic, nutrient and chlorofluoromethane data. Deep-Sea Research Part I-Oceanographic Research Papers 40, 267-291

Ribas-Ribas, M., Gómez-Parra, A., Forja, J.M., 2011. Air-sea CO_2 fluxes in the north-eastern shelf of the Gulf of Cádiz (southwest Iberian Peninsula). Marine Chemistry 123, 56-66

Ríos, A.F., Fraga, F., Pérez, F.F., 1989. Estimation of coefficients for the calculation of "NO", "PO" and "CO", starting from the elemental composition of natural phytoplankton*. Scientia Marina 53, 779-784

Ríos, A.F., Pérez, F.F., Fraga, F., 1992. Water masses in the upper and middle North-Atlantic Ocean East of the Azores. Deep-Sea Research Part I-Oceanographic Research Papers 39, 645-658

Ríos, A.F., Pérez, F.F., Fraga, F., 2001. Long-term (1977-1997) measurements of carbon dioxide in the Eastern North Atlantic: evaluation of anthropogenic input. Deep-Sea Research Part II-Topical Studies in Oceanography 48, 2227-2239

Sabine, C.L., Feely, R.A., Gruber, N., Key, R.M., Lee, K., Bullister, J.L., Wanninkhof, R., Wong, C.S., Wallace, D.W.R., Tilbrook, B., Millero, F.J., Peng, T.H., Kozyr, A., Ono, T., Rios, A.F., 2004. The oceanic sink for anthropogenic CO_2. Science 305, 367-371

599 Santana-Casiano, J.M., González-Davila, M., Laglera, L.M., 2002. The carbon dioxide
600 system in the Strait of Gibraltar. Deep-Sea Research Part II-Topical Studies in
601 Oceanography 49, 4145-4161
602 Sarmiento, J.L., Gruber, N., 2002. Sinks for anthropogenic carbon. Physics Today 55,
603 30-36
604 Schneider, A., Tanhua, T., Körtzinger, A., Wallace, D.W.R., 2010. High anthropogenic
605 carbon content in the eastern Mediterranean. Journal of Geophysical Research-Oceans
606 115, 11
607 Serra, N., Ambar, I., 2002. Eddy generation in the Mediterranean undercurrent. Deep-
608 Sea Research Part II-Topical Studies in Oceanography 49, 4225-4243
609 Takahashi, T., 2009. Climatological mean and decadal change in surface ocean pCO_2,
610 and net sea-air CO_2 flux over the global oceans. Deep-Sea Research Part II-Topical
611 Studies in Oceanography 56, 554-577
612 Tanhua, T., Jones, E.P., Jeansson, E., Jutterstrom, S., Smethie, W.M., Wallace, D.W.R.,
613 Anderson, L.G., 2009. Ventilation of the Arctic Ocean: Mean ages and inventories of
614 anthropogenic CO_2 and CFC-11. Journal of Geophysical Research-Oceans 114
615 Touratier, F., Azouzi, L., Goyet, C., 2007. CFC-11, Delta C-14 and H-3 tracers as a
616 means to assess anthropogenic CO_2 concentrations in the ocean. Tellus Series B-
617 Chemical and Physical Meteorology 59, 318-325
618 Touratier, F., Goyet, C., 2004a. Definition, properties, and Atlantic Ocean distribution
619 of the new tracer TrOCA. Journal of Marine Systems 46, 169-179
620 Touratier, F., Goyet, C., 2004b. Applying the new TrOCA approach to assess the
621 distribution of anthropogenic CO_2 in the Atlantic Ocean. Journal of Marine Systems 46,
622 181-197
623 van Aken, H.M., 2000. The hydrography of the mid-latitude northeast Atlantic Ocean I:
624 The deep water masses. Deep-Sea Research Part I-Oceanographic Research Papers 47,
625 757-788
626 Vázquez-Rodríguez, M., Padín, X.A., Ríos, A.F., Bellerby, R.G.J., Pérez, F.F., 2009a.
627 An upgraded carbon-based method to estimate the anthropogenic fraction of dissolved
628 CO_2 in the Atlantic Ocean. Biogeosciences Discussions 6, 4527–4571
629 Vázquez-Rodríguez, M., Touratier, F., Lo Monaco, C., Waugh, D.W., Padín, X.A.,
630 Bellerby, R.G.J., Goyet, C., Metzl, N., Ríos, A.F., Pérez, F.F., 2009b. Anthropogenic
631 carbon distributions in the Atlantic Ocean: data-based estimates from the Arctic to the
632 Antarctic. Biogeosciences 6, 439-451

Winkler, L.W., 1888. Die Bestimmung des im Wasser gelösten Sauerstoffes. Berichte der deutschen chemischen Gesellschaft 21, 2843-2854

Fig. 1 Map of the location of the Gulf of Cadiz and the Strait of Gibraltar and sampling grid during the P_3A_2 cruise.

Fig. 2 θ/S diagram of the study area from 100 dbar depth to the bottom: a) CTD data. Red stars represent the water types (WT) for the different water bodies (NACW, NADW and MOW) used for the eOMP analysis; b) A_T (µmol kg^{-1}); c) AOU (µmol kg^{-1}); d) C_T (µmol kg^{-1}). Contour lines represent density anomaly expressed in kg m^{-3}.

Fig. 3 Vertical distributions of a N-S transect from 100 dbar to the bottom: a) Map of the selected stations; b) Salinity; c)Potential temperature (ºC), d) Total Alkalinity (A_T) in µmol kg^{-1}, e) Total Inorganic Carbon (C_T) in µmol kg^{-1} and e) Apparent Oxygen Utilization (AOU) in µmol kg^{-1}.

Fig. 4 Vertical distributions of an E-W transect from 100 dbar to the bottom: a) Map of the selected stations; b) Salinity; c)Potential temperature (ºC), d) Total Alkalinity (A_T) in µmol kg^{-1}, e) Total Inorganic Carbon (C_T) in µmol kg^{-1} and e) Apparent Oxygen Utilization (AOU) in µmol kg^{-1}.

Fig. 5 Vertical distributions of a N-S transect from 100 dbar to the bottom: a-c) Estimates of C_{ANT} (µmol kg^{-1}) from the φC_T^o, ΔC^* and $TrOCA_{2007}$ methods respectively; d-f) percentage of NACW, NADW and MOW obtained by the eOMP analysis.

Fig. 6 Vertical distributions of an E-W transect from 100 dbar to the bottom: a-c) Estimates of C_{ANT} (µmol kg^{-1}) from the φC_T^o, ΔC^* and $TrOCA_{2007}$ methods respectively; d-f) percentage of NACW, NADW and MOW obtained by the eOMP analysis.

Table 1. Biogeochemical characteristics of the water types selected as end-members in the eOMP analysis.

	NACW		**NADW**	**MOW**
	WT1	**WT2**	**WT3**	**WT4**
Θ (ºC)	17.3	11.3	2.4	13.1
S	36.50	35.55	34.93	38.50
O_2 (µmol $kg^{-1)}$	217	179	235	167
Si (µmol kg^{-1})	0.1	7.7	22.8	9.9
NO_3 (µmol kg^{-1})	2.05	15.56	20.55	10.81
PO_4 (µmol kg^{-1})	0.16	1.14	1.39	1.20
A_T^o (µmol kg^{-1})	2362	2327	2300	2581
ΔC_{dis} (µmol kg^{-1})	-17	-6	-8	0

.

Table 2. Specific C_{ANT} inventories in the area and the specific Mediterranean contribution (number of stations used=31, surface area=14,082 Km^2).

Method	Specific Inventory (mol C m^{-2})	Contribution of MOW to the specific inventory (%)
φC_T^o	33.5±3.2	8
ΔC^*	34.2±3.2	8
$TrOCA_{2007}$	33.7±3.0	11
$TrOCA_{2004}$	38±3.1	12

Figure1

Click here to download high resolution image

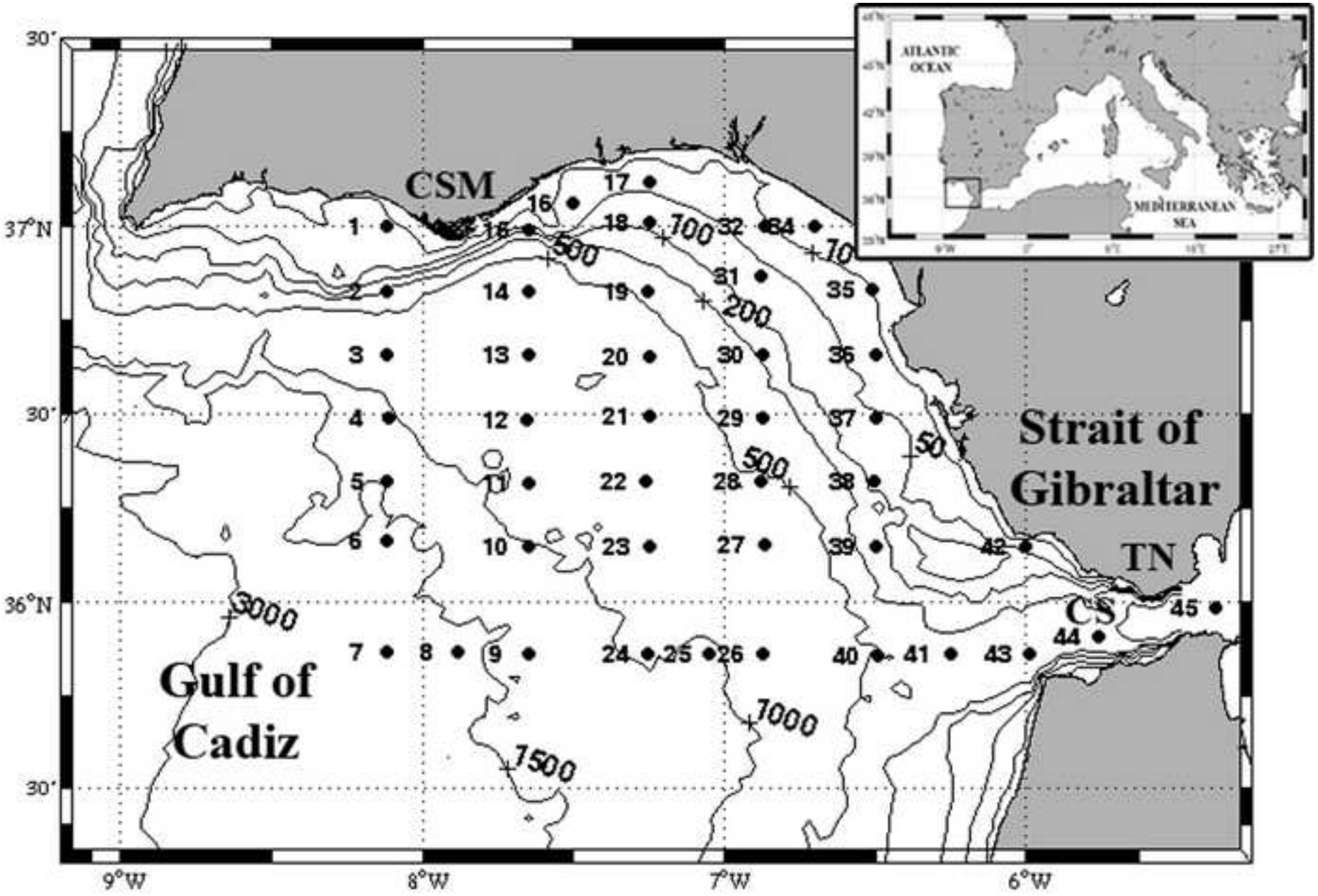

Figure2

Click here to download high resolution image

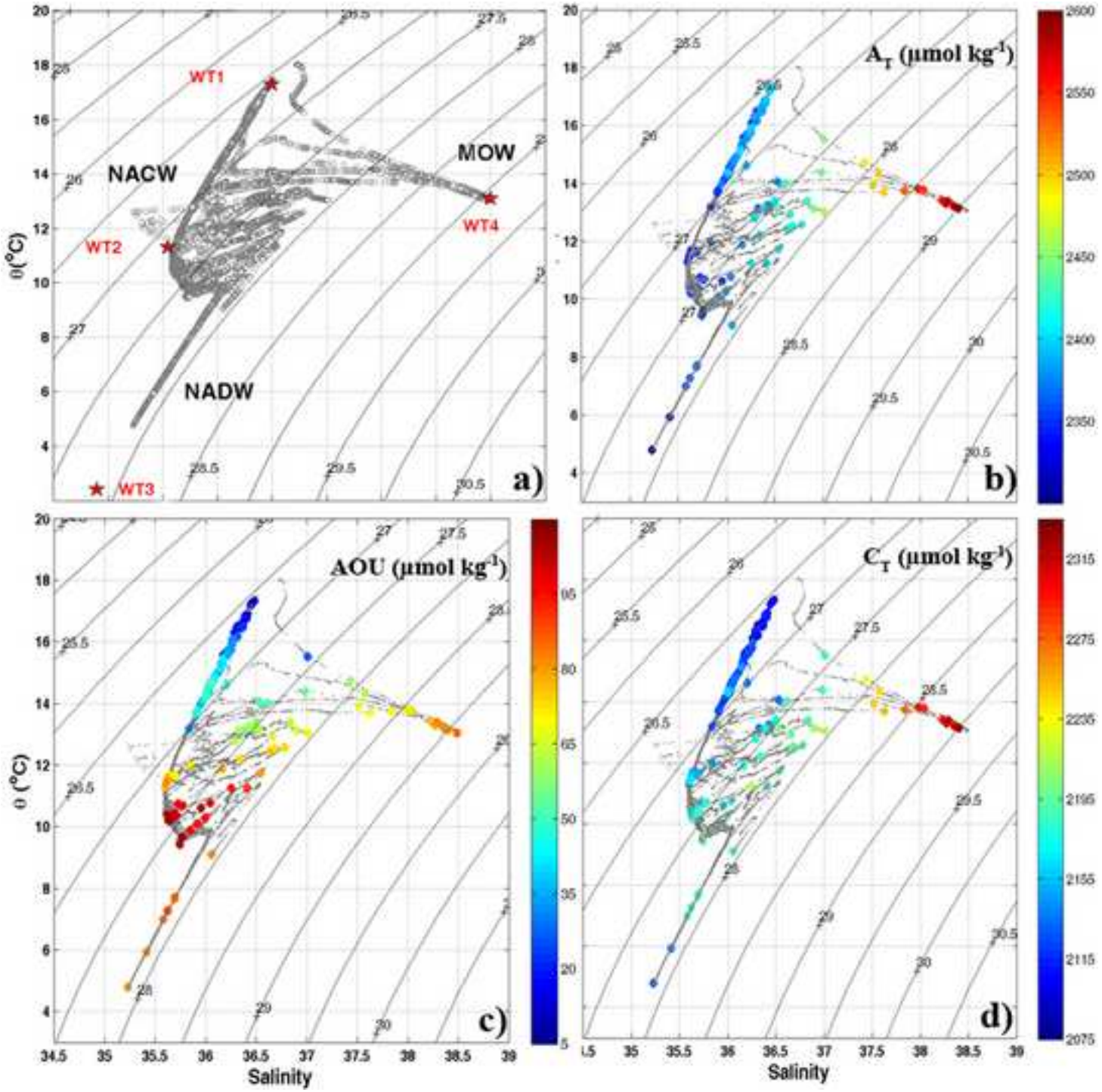

Figure3

Click here to download high resolution image

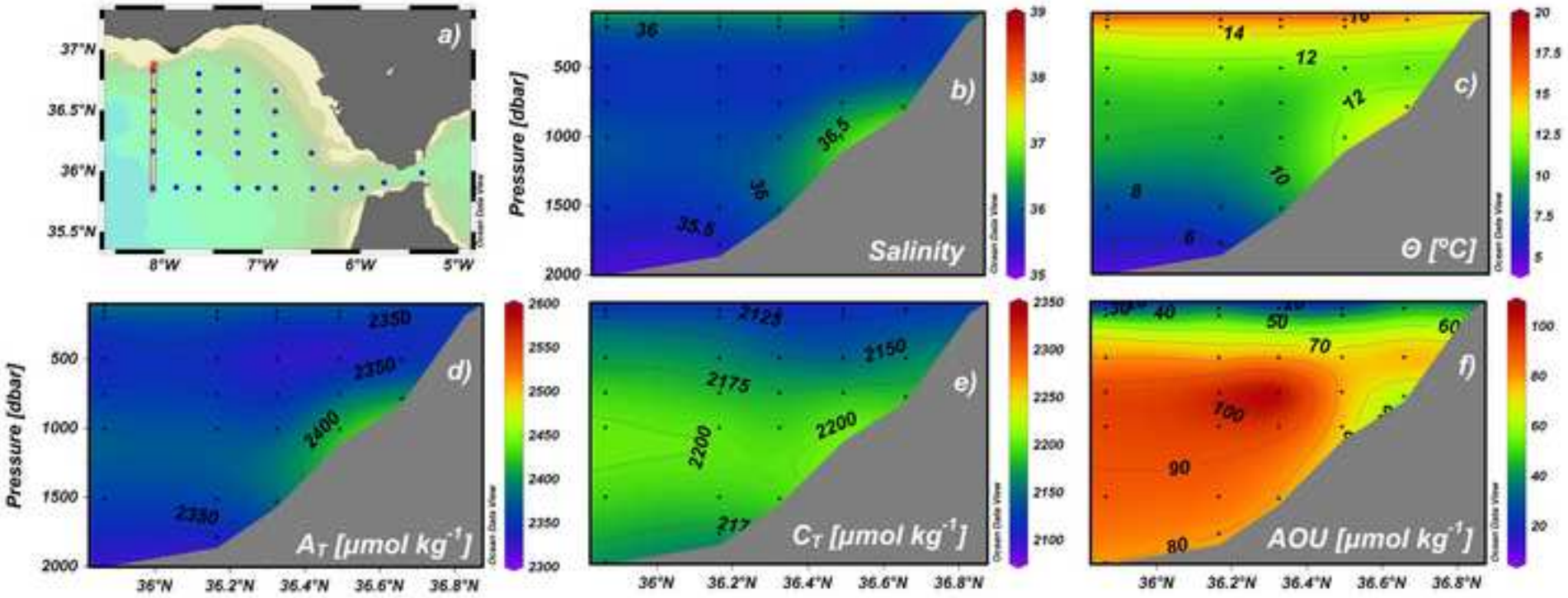

Figure4

Click here to download high resolution image

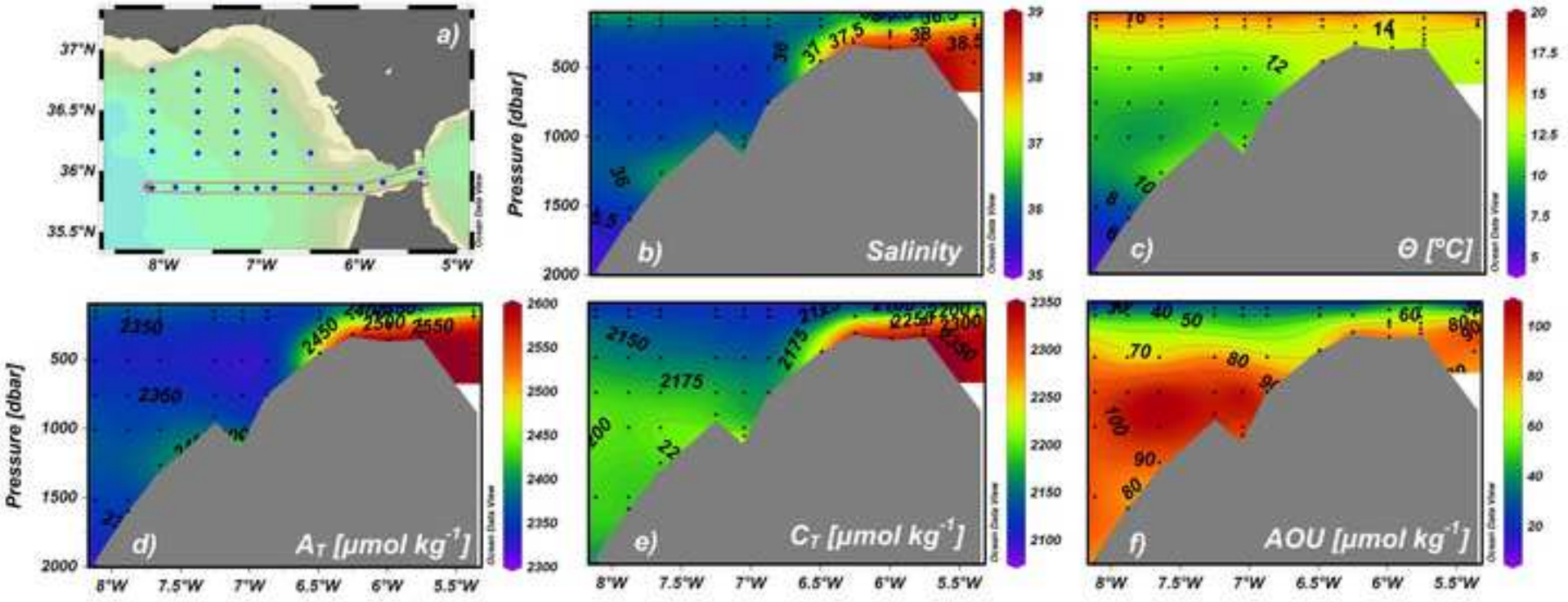

Figure5

Click here to download high resolution image

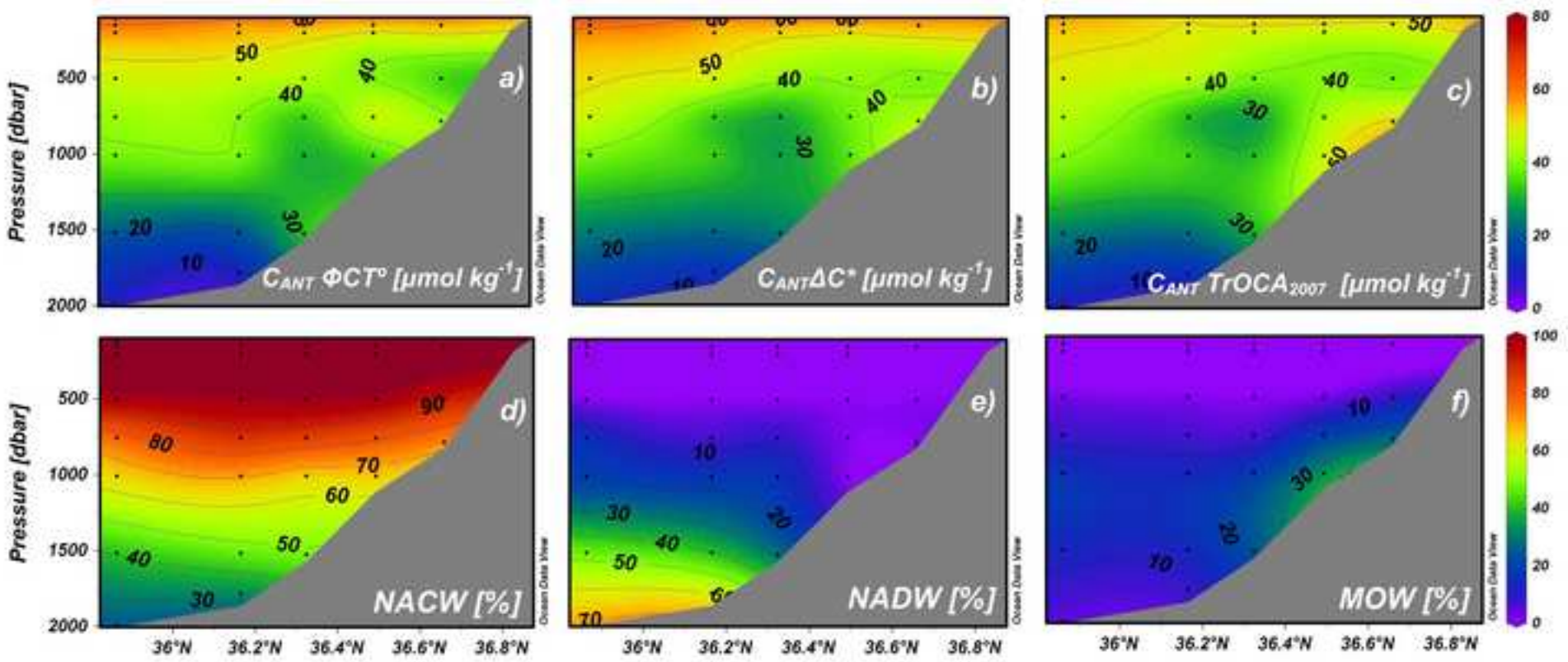

Figure6

Click here to download high resolution image